

DISPERSION EFFECTS OF SHALLOW WATER GRAVITY WAVES

Nikolai Speranski

Shirshov Institute of Oceanology, Moscow, RUSSIA

Fritz Büsching

Bielefeld University of Applied Sciences, Minden, GERMANY

Summary

Anomalous dispersion was found as a growing of the phase velocity of high-frequency bound components of shoaling gravity waves. The velocities of those components get bigger than that of the primary by up to 25% in the near shore zone, where wave heights are approximately equal to the water depth. The effect thus contradicts the theoretical conception about non-dispersive motion as a limited case of shallow water wave movement depending on water depth only. According to the observations the anomalous dispersion effect (ADE) gets weaker with the water depth decreasing and the motion is found to be non-dispersive for bore-like structures in the surf zone. The effect had been detected by field measurements when deep sea storm waves had a narrow spectrum. In laboratory measurements initially monochromatic waves of periods 2.0 to 5.0 s and heights of 0.14 m shoaled over up-sloping plane bottom. The laboratory experiments do confirm the existence of the ADE. In particular the measurements show an increase of the intensity of the ADE with the wave periods also increasing. As a result of both investigations it is found that the ADE represents a nonlinear effect, which appears, however, to be hidden at conditions characterized by free components coinciding with bound components in the same spectrum. The anomalous dispersion effect is responsible for the transformation of waves into the so-called „saw-tooth“ form being a typical feature of the surf zone.

1. Introduction

Phase velocity of shoaling and breaking waves was in focus of interest at the end of the 1970s and in the beginning of the 1980s. At that time several research groups carried out a number of field measurements on phase velocity (or celerity) in the near shore zone in the depth range 0.5 m - 7.0 m. (Büsching, 1978; Thornton and Guza, 1982; Elgar and Guza, 1985). The main characteristic discussed was the so-called "celerity spectrum" defined as the re-

lation between the phase velocity C of wave components and frequency f according to formula

$$C(f) = \frac{X_{12}}{\varphi_{12}(f)/2\pi f} \quad (1)$$

where X_{12} is the distance between measuring stations 1 and 2 and φ_{12} is the phase difference between the harmonics of frequency f at those stations.

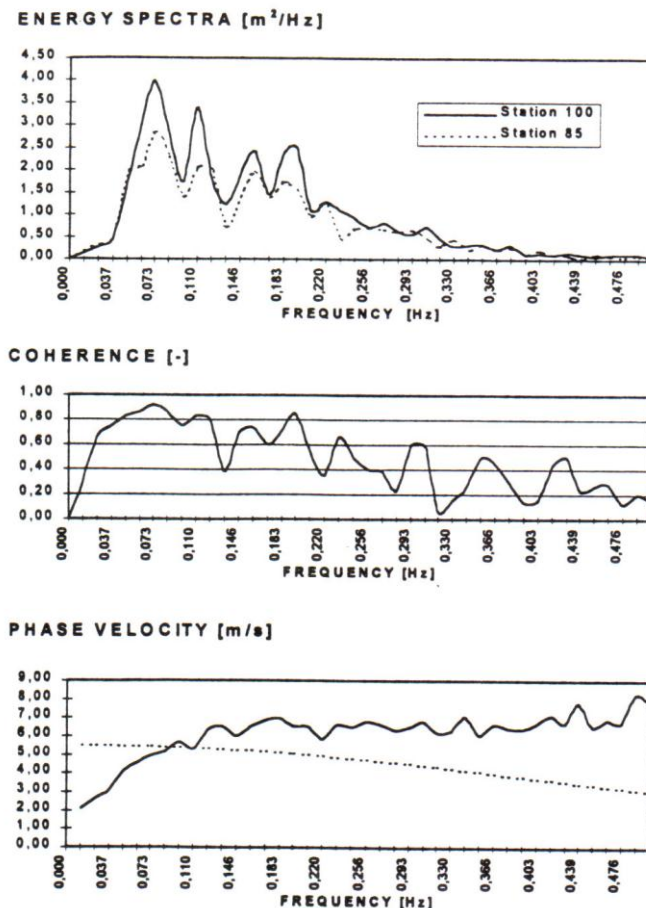


Fig.01: Energy spectra, coherence function and celerity spectrum at storm surge conditions of December 14, 1973. Sylt Island, North Sea. The theoretical phase velocity curve is marked by the dashed line (Büsching, 1978).

have the following features:

In relatively deep water, where nonlinear effects are weak, the function $C(f)$ decreases when frequency grows, in consistence with linear theory.

In shallow water the discrepancy increases between theoretical and measured magnitudes of the celerity in the onshore direction, because measured spectra tend to some constant value (Thornton and Guza, 1982).

S. Elgar and R. Guza presented measuring data demonstrating the growth of high harmonics of shoaling waves as a result of intensive nonlinear interactions between high harmonics and the primary as well as between high harmonics mutually. It had been proved experimentally that in the case of a narrow spectrum in deep water (input conditions), high harmonics of shoaling waves may be classified as bound components (Elgar and Guza, 1985). The process of generating nonlinear harmonics starts to show the property of accumulation, when waves achieve sufficiently shallow water where the Ursell number is bigger then 16 (Lighthill, 1978; Speranski, 1986). E. Thornton and R. Guza found by field measurements that celerity spectra

However, almost at the same time several strange spectra from shoaling and surf zone waves were found revealing increasing phase velocities with the frequency increasing (Fig.01). This increase appeared in the frequency range $f \geq f_2$; the index denoting the number of the harmonic.

First this type of spectra was measured at Sylt island, North sea (Büsching, 1978). Several years later similar spectra were measured at the Pacific coast (Elgar and Guza, 1985). A set of such spectra was also obtained in measurements at the Black Sea coast (Kuznetsov and Speranski, 1990). It is of interest to note that the data of Thornton and Guza, mentioned above, also reveal this feature, but only as a very weak effect. In fact these spectra reveal an anomalous property of gravity waves in shallow water, which is beyond the scope of knowledge about wave kinematics.

Table 1: Characteristics of abnormal celerity spectra

Author(s)	Year	Place	Intensity (%)	Error (%)
Büsching	1978	The North Sea Sylt Island	$I_{21} = 25-32$	± 11
Elgar, Guza	1985	The Pacific Ocean California	$I_{31} = 5-10$ ($f = f_3$)	± 9
Kuznetcov, Speranski	1990	The Black Sea Schcorpilovzci	$I_{21} \approx 5$ ($f = f_2$)	± 8
Thornton, Guza	1982	The Pacific Ocean California	$I_{21} \approx 0$	± 5

Table 1 contains some characteristics of the anomalous spectra. The first three columns do not need to be explained. The fourth column contains the magnitudes of relative differences I_{j1} of the celerity, defined as

$$I_{j1} = \frac{C(f_j) - C(f_1)}{C(f_1)}, (j \geq 2) \quad (2)$$

where j is a harmonic number.

Measured values of I_{21} attain 0.32 (Table 1), and this suggests the existence of a new effect, which might be named "High-frequency anomalous dispersion of bound waves propagating on shallow water". The term "high frequency" means the frequency range $f > f_1$; the condition $f < f_1$ defines the "low frequency" range. However, in all papers mentioned above, there are no data about the accuracy of the measurements, and therefore the existence of the effect is doubted.

In order to ascertain the existence of the phenomenon, it is necessary to evaluate the errors in the determination of the celerity spectra and check them with the corresponding magnitudes of I_{j1} .

If this effect exists, it could explain the positive (and shoreward increasing) shift between high harmonics and the primary one, when waves shoal over up-sloping bottom (Flick et al., 1981); i.e. one of the most important features of wave deformation in the surf zone, causing the formation of bore-like structures.

The first aim of this paper is to ascertain, whether the anomalous dispersion effect ("AD-effect") takes place in shallow water waves (both in regular and irregular waves), and if so, to estimate the intensity of the phenomenon and to study the conditions of its appearance. The second problem of the article deals with the properties of celerity spectra in the low frequency range. The point is that the measurements at Sylt island also comprised spectra showing anomalous properties at low frequencies (Fig.01): At the frequency 0.04 Hz the celerity is about 50% less than that at the frequency of 0.07 Hz (Büsching, 1978) This phenomenon radically contradicts to all theories of gravity waves, which predict the growing of phase velocities with the frequency decreasing.

In this place it has to be noted that the experiments at Sylt island had been conducted at conditions of severe storm and high storm surge. Therefore it is of importance to check this low-frequency effect for conditions of moderate waves ("usual storms") and especially for swell conditions, when the influence by wind is negligible. It is well known that low-frequency oscillations of the sea level control such phenomenon as *surf beats*. Therefore the study of low-frequency wave kinematics is of importance for the understanding of the mechanisms of wave deformation in the surf zone.

Thus both effects probably are responsible for the development of waves in the surf zone: the high-frequency anomalous dispersion leads to the generation of sawtooth wave profiles, i.e. bore-like structures, whereas the low-frequency effect can have an influence on the generation of surf beats. As both effects are sufficiently unusual and contradictive to theory, this circumstance should stimulate to accurate checking them.

The problems formulated are solved in the way of estimating the errors of previous measurements (to check the correctness of conclusions) as well as by the analysis of new measurements of field and laboratory conditions.

2. Errors of celerity measurements

The total error of celerity measurements consists of two independent parts:

- the error in the determination of $C(f)$ by formula (1) and

- the error due to the action of *undertow flow* and *angular spreading* of the wave spectrum.

It can be shown easily from (1) that the error in the determination of the celerity is established by formula

$$\frac{\Delta C}{|C|} = \frac{\Delta X}{|X|} + \frac{\Delta \varphi}{|\varphi_{12}|} \quad (3)$$

where the absolute error is denoted by the symbol " Δ ".

The first term on the right side of (3) is usually of the order of 1%. The value of φ_{12} can be found in using the method of cross-spectral analysis, and in that case it depends on the number of degrees of freedom as well as on the magnitude of the coherence function for a particular frequency. The plot on Fig.02 demonstrates this relation.

Calculations of errors for cases mentioned above show that the determination of

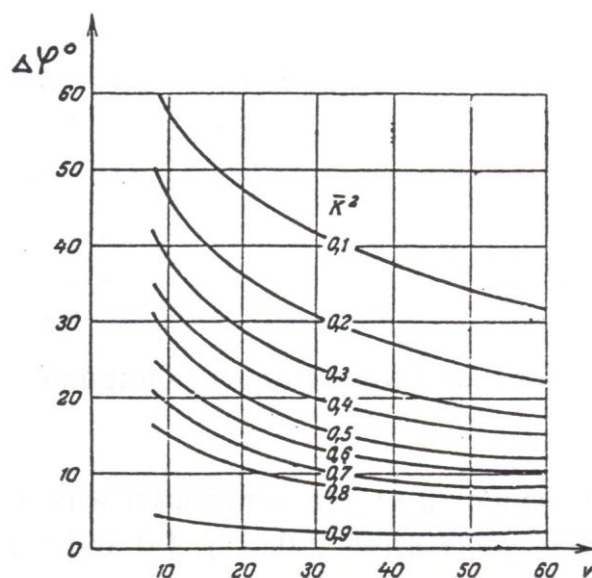


Fig.02: 95%-confidence interval ($\Delta\varphi$) for phase spectrum as a function of degree of freedom (ν) and coherence (κ). By Jenkins and Watts (1968).

sion (4th column of Table 1) shows that I_{j1} and $\Delta C/C$ are values of the same order. The celerity spectra measured at Sylt island are the only exception. This means that it is necessary to consider additional data to confirm the existence of the AD-effect.

As to the low-frequency effect, the corresponding error of the celerity measurements at frequencies $f < 0.08$ Hz is in the range of 10% to 20% (depending on the variation of the coherence function, ref. Fig.01 and Fig.02), whereas the

phase by cross-spectral method is quite accurate. The data for the calculation of the water depth and the spectral peak frequency have been taken from the original papers. The phase shift was calculated according to $2\pi X_{12}/L_j$, where the length of the j -harmonic is $L_j = (gD)^{1/2}/f_j$. The error due to the influence of undertow flow (that has off-shore direction and speed of the order of 0.1 m/s) and the angle spreading do not exceed 2-3% (Thornton and Guza, 1982). The total error values calculated do not exceed 11% (column 5 of Table 1).

However, the comparison of these values with the measured intensity of anomalous disper-

intensity of the effect is equal to about 50% (Fig.01). Hence there is no doubt with respect to the measurements of this frequency range.

3. Flume measurements

Laboratory measurements were conducted at the wave flume of Qingdao Ocean University, China, in 1990. The main dimensions of the flume are as follows: length 40 m, width 1.2 m and depth in the horizontal section 0.70 m. The slope 1:33 was modeled in using an inclined plane section made of steel sheets (Fig.03).

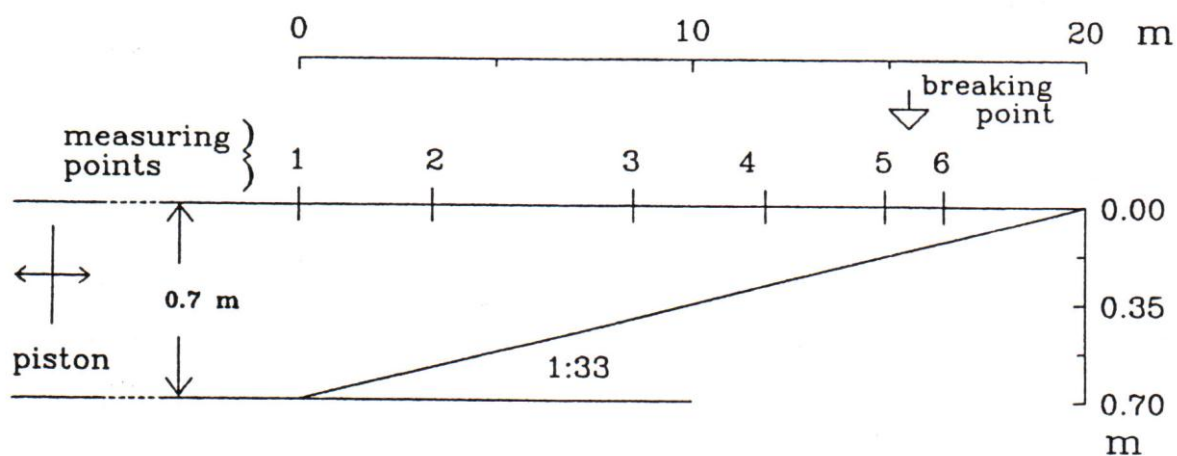


Fig.03: Scheme of laboratory measurements in the wave flume of Qingdao Ocean University

A piston type wave maker was used for producing regular sinusoidal waves of stable heights in the range of 0.14 - 0.16 m and periods 2.0, 3.0, 4.0 and 5.0 s. For the synchronous measurement of surface elevations six capacitance type wave gauges were placed at distances one to another 1.5 m to 5.1 m (Fig.03, Table 2). The sampling rate was equal to 10 Hz.

Table 2: Location of wave gauges at flume measurements.

Point	1	2	3	4	5	6
Depth (m)	0.70	0.61	0.45	0.32	0.22	0.17
Distance (m)	0.00	3.38	8.48	12.36	15.41	16.91
Distance between gauges (m)		3.38	5.10	3.88	3.05	1.50

Waves of period 2 s demonstrate the sinusoidal form and appropriate spectrum with the only narrow peak at the initial point at the toe of the upsloping section (point 1 in Fig.03) whereas waves of periods $T \geq 3$ s show new peaks at multiple frequencies ($f_j = j \cdot f_1$) resulting from shoaling over the horizontal section 20 m long (Fig.04).

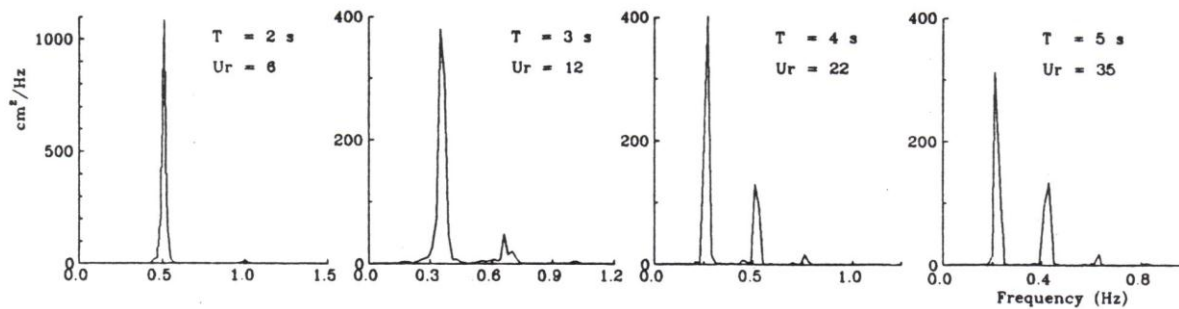


Fig.04: Spectral density of surface elevations at the toe (initial point p1) of the upsloping section. Wave periods 2 s, 3 s, 4 s and 5 s.

The Ursell number (Ur) is used to characterize the nonlinearity of waves at the respective measuring station 1. This number is the ratio of the nonlinear term in the Korteweg-de Vries equation (proportional to H/D) to dispersion term (proportional to $(D/L)^2$) and therefore it can be used as a quantity deciding on the degree of nonlinearity-dispersivity of the wave motion. H and L denote wave height and length, D is a local water depth. In the common form mentioned in the Introduction, Ursell number is expressed as

$$Ur = 0.5 \frac{HL^2}{D^3} \quad (4)$$

The corresponding values of Ur presented in Fig.04, mean the growth of nonlinearity of waves at the initial point 1, when the wave period increases. This feature is illustrated also by new spectral peaks. The specific case of wave deformation over up-sloping bottom is shown in Fig.5, where the measured time-series represent surface elevations of period $T = 4$ s at all six measuring stations.

The observations have shown that waves broke as spilling, spilling-plunging or plunging (in accordance with the period) in the narrow zone between points 5 and 6, which is situated 3-4 m apart from the point of intersection of the still water level with the slope face. At stations 1 through 4 very stable waves could be watched all over the measuring period, whereas at stations 5 and 6 there are superimposed slight low-frequency oscillations of the period of about 30s (Fig.05).

Celerity spectra were calculated in using formula (1), where the quantity ϕ_{12} was determined by the method of cross spectral analysis of two time series $\eta_1(t)$

and $\eta_2(t)$ measured at 2 neighboring stations. The width of the spectral window and the number of degrees of freedom were equal to 0.05 Hz and 34 respectively.

The main result of the flume measurements is introduced by Fig.06 as the relationship $C_1(X)$ and $C_2(X)$, where X is a horizontal distance from the origin of the sloping section and the index denotes the harmonic number. Those sets of curves demonstrate the similar behavior of waves of all periods measured. At the section between points 1 and 2 the celerity of the first harmonic exceeds that of

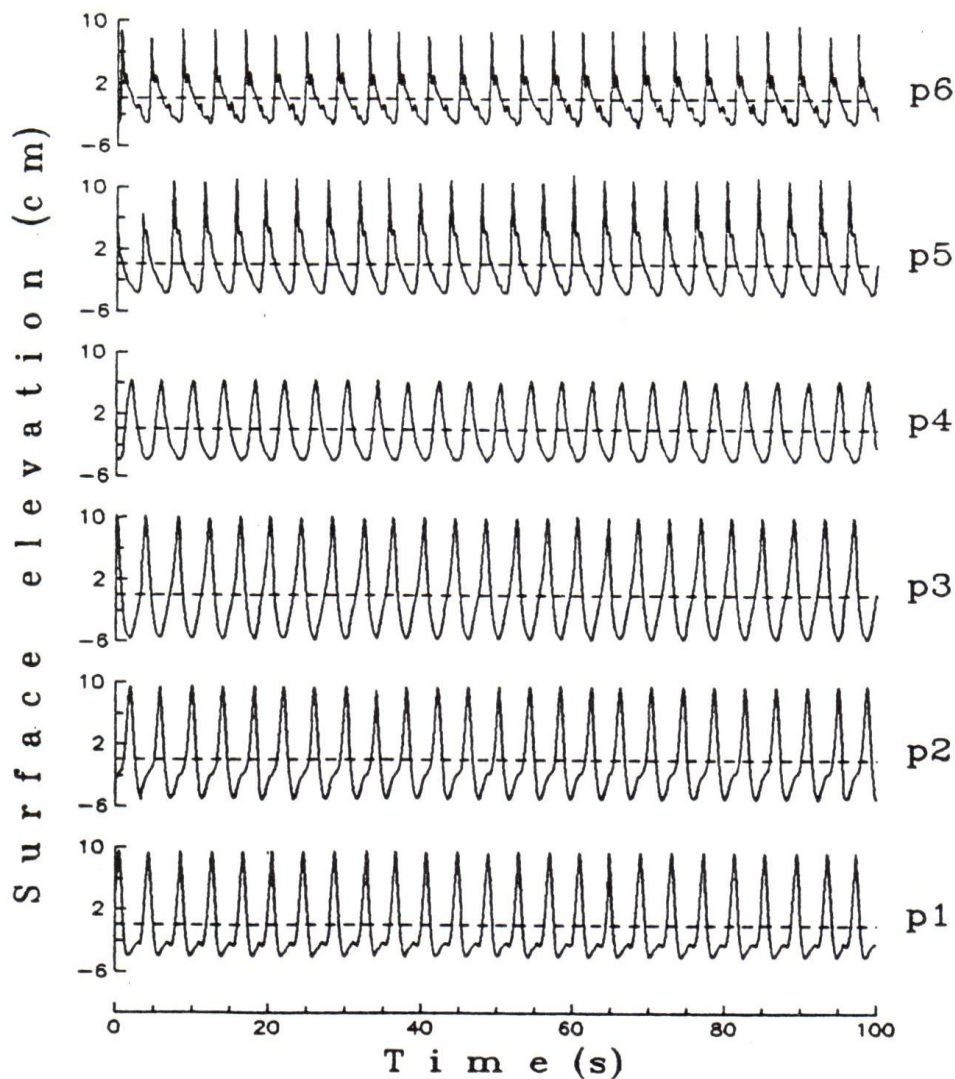


Fig.05: Time-series of waves shoaling over the up-sloping section ($T = 4$ s). Measuring stations are denoted p1 through p6.

the second harmonic, demonstrating normal dispersion of gravity waves. Shoreward between points 2 and 3 the values of C_1 and C_2 get closer and finally the intersecting curves point out a non-dispersive motion inside this interval. This is true for waves of periods $T = 2$ s, 3 s and 4 s. In the case of waves of period $T = 5$ s the dispersionless section is displaced shoreward (between points 4 and 5; Fig.06). Onshore of this section (between points 3 and 5) the celerity of the second harmonic steadily exceeds the corresponding value of the primary harmonic (anomalous dispersion). The maximum positive value $C_2 - C_1$ is found between points 3 and 4 (Fig.06), except for the waves of period $T = 5$ s. In the further onshore direction this quantity decreases and between points 4 and 6 (for $T = 2$ s and 3 s) or between points 5 and 6 (for waves $T = 4$ s) it is of the order of error of the measurement. Waves of period $T = 5$ s demonstrate anomalous dispersion between points 5 and 6, i.e. in the breaking zone.

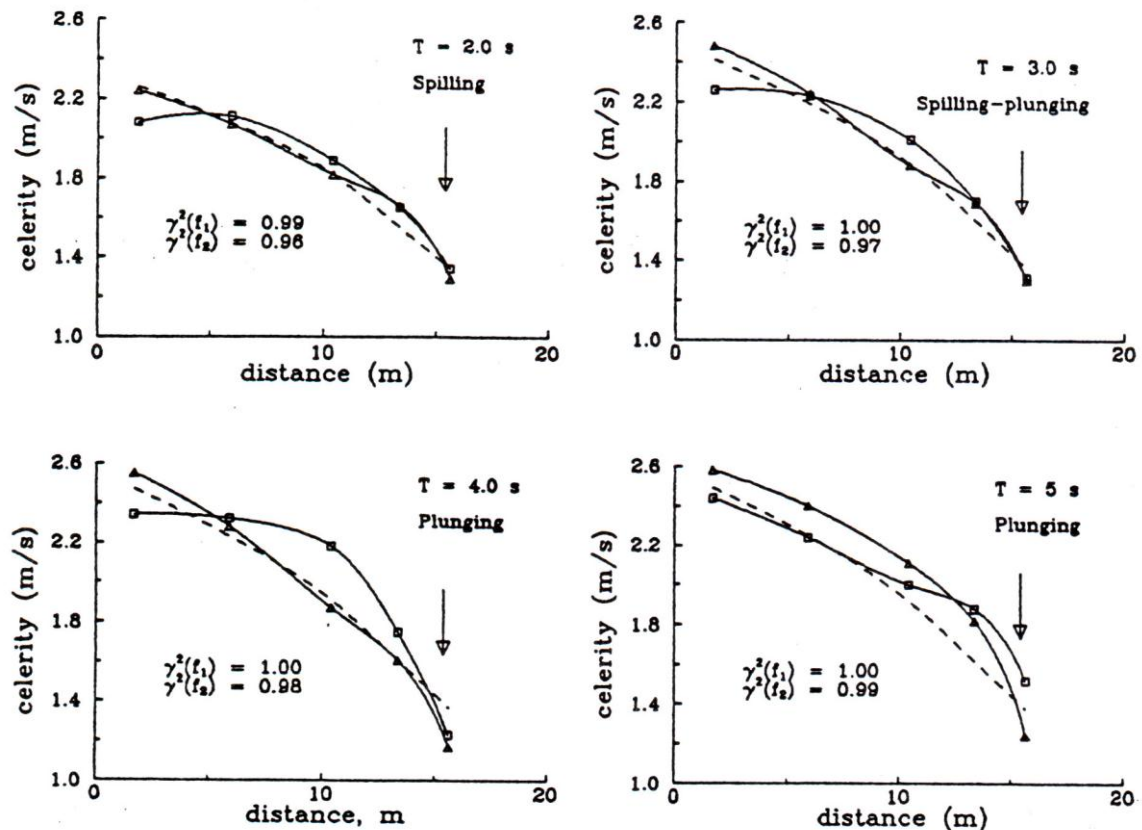


Fig.06: Variation of the phase velocity of regular waves propagating over sloping bottom: the celerity of the primary harmonic is denoted by triangles, the celerity of the second harmonic is denoted by squares. The dashed line shows calculated values by linear theory. The arrow indicates the wave breaking position.

With respect to the accuracy of the celerities of the flume experiments the total error was determined (as explained above) to be less than 5% in any case.

The value of the intensity of the AD-effect is smallest ($I_{21} \approx 4\%$) for the wave of period $T = 2$ s, whose second harmonic is rather weak. But with respect to wave periods $T = 3$ s, $T = 4$ s and $T = 5$ s the corresponding values are 7%, 17%, and 23%, meaning that the intensity increases with periods increasing. Hence, except for period $T = 2$ s for all the runs the criterion of a bigger intensity than the estimated error is fulfilled; at the wave period $T = 5$ s the respective percentage value is even more than 4 times bigger.

This, in fact, confirms strictly the existence of high-frequency anomalous dispersion in regular laboratory waves.

4. Field measurements

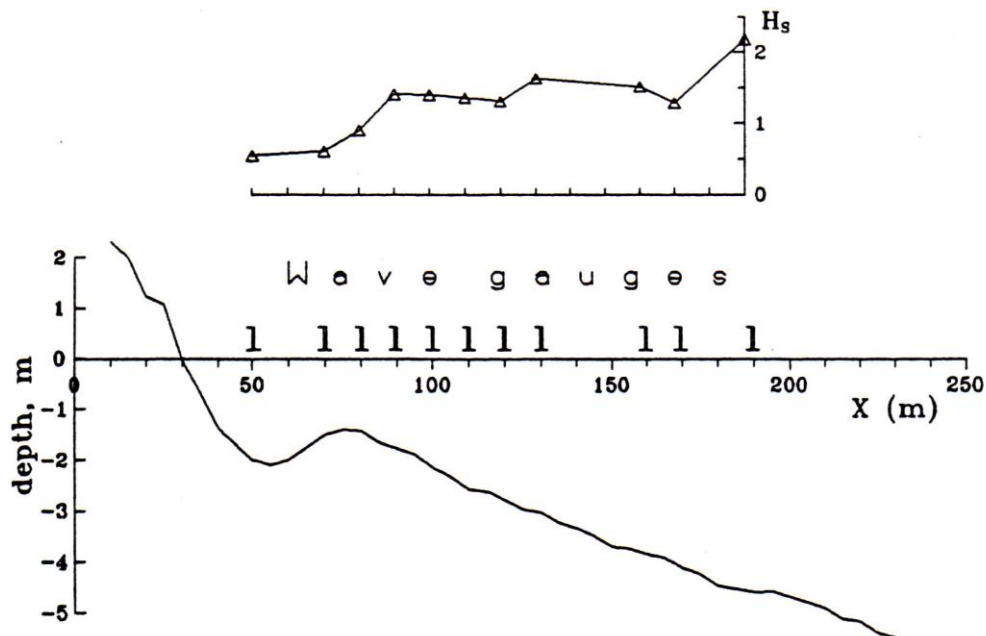


Fig.07: Scheme of field measurements at Schcorpilovzci research pier, at the Black sea coast. Bottom profile and the positions of the wave gauges are shown in the lower panel and the variation of the significant wave height in the upper panel.

Field measurements were carried out in October 1985 at Schcorpilovzci site at the Black Sea coast near Varna City, Bulgaria. The research pier of the Bulgarian Institute of Oceanology is situated at a sandy coast partition, 12 km long; and the measuring profile is located 4 km from its southern end. The beach disposes

of almost parallel bottom contours with the average slope 0.02. The average size of the beach material is 0.2 mm (fine sand). The area of the measurements extended from the 0.5 m contour line to the 5.0 m contour line. In the period of the observations the beach profile had a single underwater bar, whose top was at a distance of 45 m from the shoreline (Fig.07). The tidal oscillations are less than 0.1 m. Resistance type wave gauges were used to measure surface elevations at 11 points simultaneously. Further offshore in the same measuring profile two additional wave gauges were positioned on special observation towers. The first tower was at a depth of 18 m ($X = 1000$ m) and the second tower at a depth of 10 m ($X = 600$ m, where X is the distance from the origin of the coordinate system, which is located 30 m onshore of the shoreline, ref. Fig.07).

The record length of digital data was 15 minutes for every run of measurements with the sampling frequency 3.3 Hz. The error of synchronization was less than 0.005 s. The calculation of the celerity spectra was performed in using formula (1). Phase spectra $\phi_{12}(f)$ were determined by the method of cross-spectrum analysis. The width of the spectral window was chosen to be equal to 0.03 Hz for the case of the high-frequency dispersion study ($0.08 \text{ Hz} \leq f \leq 0.50 \text{ Hz}$) and to 0.015 Hz, when the low-frequency range was analyzed.

One set (D16) of the measuring data revealing the remarkable effect of anomalous dispersion is considered in detail in this study. This run was taken at swell conditions with the waves propagating normally to the shore line. The significant wave height decreased from 2.18 m before breaking ($X = 190$ m) to 0.55 m in the inner part of the surf zone ($X = 50$ m). Breaking of the highest waves started near the point $X = 170$ m, whereas the majority of waves broke in the vicinity of the underwater bar ($X = 90\text{-}80$ m).

Wave conditions at point $X = 1000$ m ($D = 18$ m) may be considered as input ones. The surface elevations at this point had a single-peaked ($f_1 = 0.12 \text{ Hz}$) narrow spectrum. The spectrum becomes wider when waves shoal. This phenomenon is observed first at point $X = 600$ m ($D = 10$ m) and at all points of the measuring section (Fig.07).

The first reason of the broadening of the spectra is due to the growth of high frequency peaks at multiple frequencies. The second reason is the emergence of the peak at the frequency of about 0.04 Hz. Both effects are observed inside the whole measuring area, however, the second effect is intensive in the vicinity of underwater bar only (between the top of the bar and the point of coordinate $X \approx 120$ m).

These phenomena control both the asymmetry of shoaling waves and low-frequency oscillations, or surf beats (Fig.08). The corresponding energy spectra demonstrate the growth of high- and low-frequency peaks (Fig.09, the right panel).

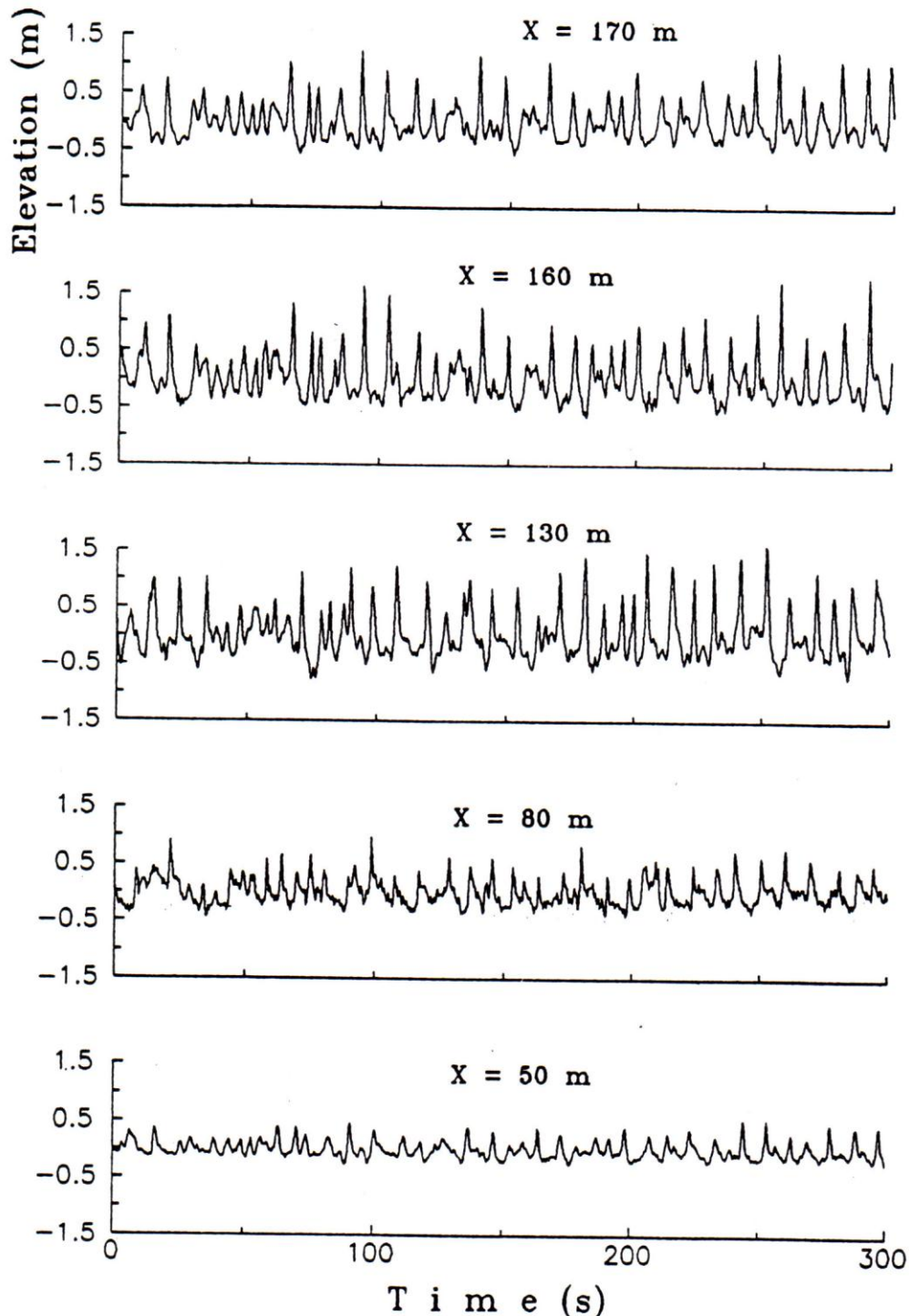


Fig.08: Time series of surface elevations measured at different points of the pier. Distances X refer to the measuring stations.

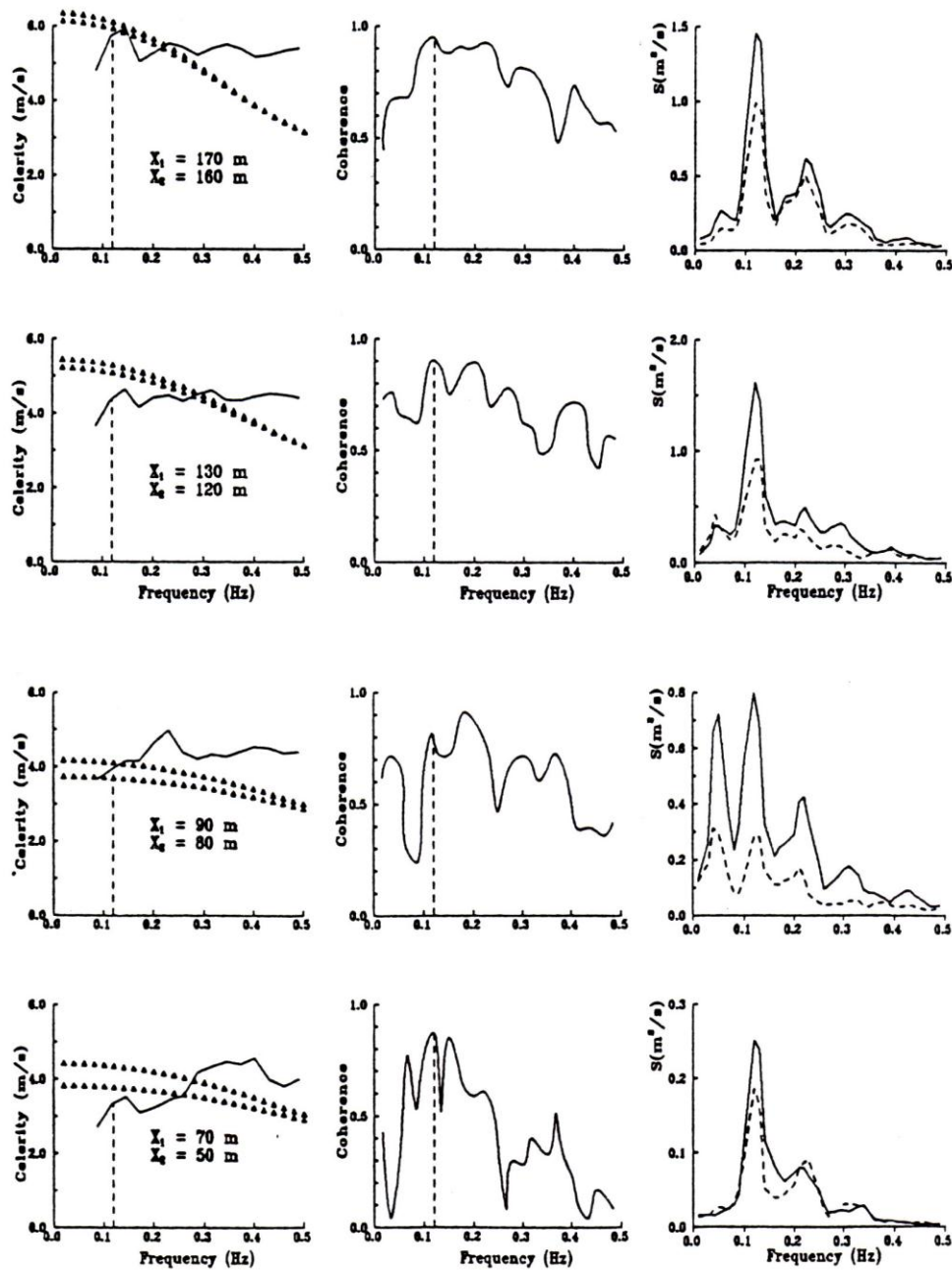


Fig.09: Celerity spectra, coherence functions and spectral density at sections $X = 170-160$ m, $X = 130-120$ m, $X = 90-80$ m and $X = 70-50$ m. The

values of the phase velocities calculated in using linear theory considering the maximum depth of each section are denoted by triangles. The frequency of the spectral peak is marked by vertical dashed lines in the celerity and coherence plots. The spectral density at the offshore stations is denoted by the solid line, the same for the onshore stations is denoted by dashed line.

Fig.09 (the left panel) demonstrates the shoreward development of the high-frequency phase velocity spectra in the range 0.08-0.50 Hz. The transfer takes place from weak normal dispersion at the section $X = 170-160$ m to dispersionless wave motion at the section $X = 130-120$ m. Further onshore one can notice the weak anomalous dispersion in waves breaking on top of the bar ($X = 90-80$ m). Finally there is a clear anomalous dispersion with intensity $I_{21} \approx 20\%$ in the trench between the bar and the beach ($X = 70-50$ m).

In order to check the reliability of the measurements in the following the error in the determination of $C(f_2)$ is estimated at section $X = 70-50$ m: The phase difference measured is 477° , the corresponding value of coherence function is 0.6 (Fig.09, the middle panel), and the degrees of freedom are 54.

For these quantities the plot in Fig.02 delivers $\Delta\phi = \pm 10^\circ$ and consequently $\Delta\phi/\phi = 2\%$. Taking into account that $\Delta X/X \approx 1\%$ and that undertow flow and angular spreading of waves additionally give 2-3% (Thornton, Guza, 1982), the total error may be found to be 5-6% only. This value is significantly less than the intensity of anomalous dispersion measured ($I_{21} \approx 20\%$). Thus it is confirmed that the high-frequency anomalous dispersion effect does exist in irregular waves in field conditions.

Low-frequency wave motion ($f < 0.08$ Hz) was observed along the whole measuring section (Fig.09). Its intensity peaks at point $X = 90$ m, i.e. very close to the top of the bar. The spectral density of surface elevations at frequencies 0.03-0.04 Hz has values of the same order as the main spectral peak.

The corresponding coherence function is about 0.8 (Fig.10). The celerity spectra in the low-frequency range reveals a sharp increase of phase velocity up to values of the order of tens or even hundreds of m/s (Fig.10). By contrast the corresponding values of the phase spectrum are extremely small (of the order of 1°). Hence, this result apparently does not confirm the low-frequency effect found by measurements at Sylt island; moreover it is quantitatively opposite to that shown in Fig.01.

5. Discussion

5.1 High-frequency range

The data presented above demonstrate the existence of high-frequency anomalous dispersion. Sometimes this is the second order effect, but in specific cases its intensity may extend 20% and more. At laboratory conditions the phenomenon is observed in regular gravity waves shoaling over up-sloping bottom. In field conditions the weak AD-effect is observed near the top of the underwater bar, however, its maximum intensity is in the trough between the bar and shoreline.

The essential feature of the effect considered is that it appears in bound waves. The statement that high harmonics are bound components may be confirmed at least by two different ways. The first way is to evaluate the bicoherence function for any triples of harmonics and use quantities found as a measure of quadratic coupling. The second way is to use the criterion $Ur \geq 16$ (Lighthill, 1978). The second method is used in this study.

The estimation of the value Ur was made above for regular wave conditions. But if irregular waves are considered, some uncertainty occurs concerning the wave height characteristic. There are several wave heights possible to be entered into the Ursell number: significant height (H_S), root mean square height (H_{rms}) or mean wave height $H = 2\sigma$, where σ is the standard deviation. Values of Ur were calculated using all the wave heights mentioned above with respect to measuring station $X = 190$ m.

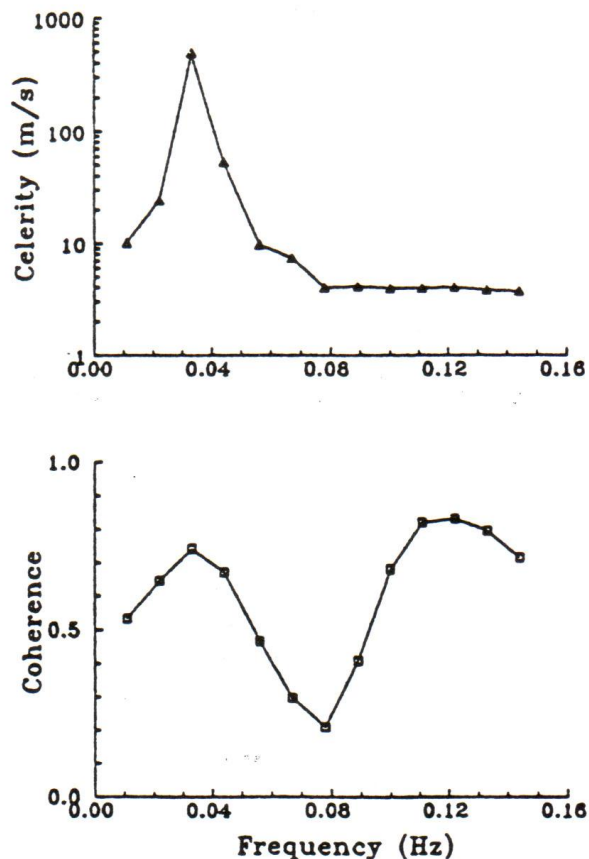


Fig.10: The celerity Spectrum (the upper) and the coherence function (the lower) at the section $X = 90$ -80 m. Low frequency range.

These quantities are as follows:

$$Ur(H_S) = 50,$$

$$Ur(H_{rms}) = 35$$

$$Ur(H_M) = 25.$$

Taking into account that H_M is the minimum characteristic of average wave height, one may conclude that the whole measuring area is a strongly nonlinear zone.

Consequently the high harmonics of energy spectra of Fig.09 are bound wave components. In turn, it means that the AD-effect is a nonlinear phenomenon, and therefore the critical conditions of its appearance may be expressed by the parameter of nonlinearity (H/D) in the Korteweg-de-Vries-equation. Such corresponding quantities of this parameter calculated for the significant wave height are presented in Table 3.

Table 3: Critical conditions of the AD-effect

Condition	Flume	Flume	Flume	Flume	Field
T (s)	2	3	4	5	8.5
H _s /D	0.4	0.4	0.4	0.8	0.8

As to the contradiction between the field data of Thornton and Guza ($C(f) = \text{constant}$ when $f \geq f_1$) and our results describing the increasing the of phase velocity between high harmonics and the primary, when waves are shoaling over

up-sloping bottom, the following question has to be answered:

Why is the AD-effect so weak or negligible in many measurements ?

It may be assumed that the width of the deep water wave spectrum plays the main part in this problem. Probably the AD effect is marked better, when the "input" spectrum is narrow. Actually a wide "input" spectrum may be considered as a set of free waves running with different phase velocities. When shoaling, every free component generates its own set of high harmonics, and as a result a wide original spectrum becomes yet wider. Some new bound components can have frequencies close to frequencies of some free waves, and the superimposition of them will attenuate the anomalous dispersion effect at the frequency of the bound components. This is a possible reason, why the AD-effect often is weak and sometimes not observed in field conditions.

It is of interest to note that in all cases considered, the AD-effect is a result of the "anomalous" (in relation to linear dependence of $C(f)$) behavior of the second harmonic and never that of the primary (Fig.06). This suggests that high-frequency anomalous dispersion is the main mechanism of wave transformation producing sawtooth waves in bore-like structures inside the surf zone. Actually a sawtooth curve may be introduced in the form

$$\xi(t) = \sum_{j=1}^{\infty} a_j \cos\left(2\pi f_j + \pi \frac{(j-1)}{2}\right) \quad (5)$$

where the term $\pi(j-1)/2$ is a positive shift between the j -harmonic and the primary one. Such high harmonics phase shift was found in the flume experiment by Flick et al. (1981). It is apparent that high harmonics of waves tending to sawtooth form have to move faster than the primary, and our laboratory measurements confirm this. Thus we should consider the high frequency anomalous dispersion to be the wave shoaling mechanism responsible for the transformation of waves into the sawtooth form (typical form of waves in surf zone). Moreover Flick's experiment demonstrated clearly that the shift considered produces the wave asymmetry relative to the vertical plane. By this reason we can state that the AD-effect is responsible for the appearance and increase of the vertical asymmetry of shoaling waves.

5.2 Low-frequency range

It was noted above that the form of the celerity spectrum measured at "Schcorpilovzci" pier in the frequency range 0.01-0.08 Hz apparently does not confirm the existence of the anomalous feature shown in Fig.01. Moreover there is an apparent discrepancy in the tendency of the spectral change: the relationship $C(f)_{\text{SYLT}}$ decreases when $f \rightarrow 0$, whereas $C(f)_{\text{SCH}}$ increases abruptly ranging up to values which seem to be physically nonrealistic (Fig.10). However, the comparison of the energy spectra of Fig.01 and Fig.09 suggest that we are dealing here with totally different phenomena. Actually, at Sylt measurements the energy densities are very small in the frequency range 0.03-0.04 Hz (Fig.01), whereas in the Schcorpilovzci measurements we have the isolated spectral peak (Fig.09). As, however, to the left section of the main spectral peak, the celerity decrease takes place in all cases measured.

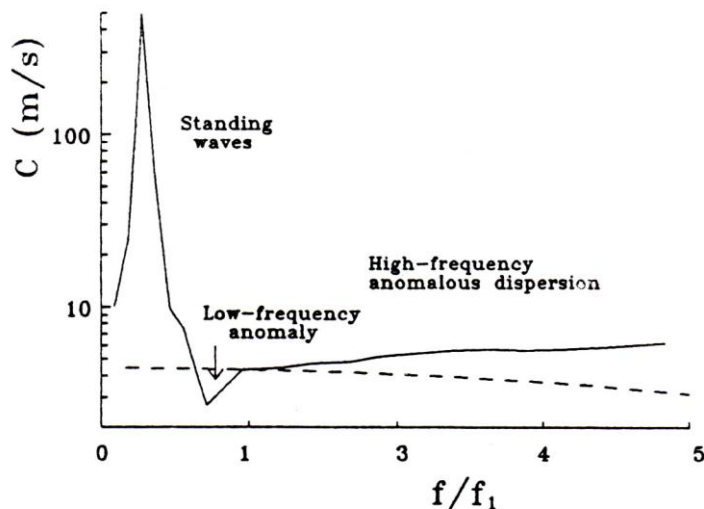


Fig.11: Generalized celerity spectrum of strongly deformed and breaking waves (solid line) in comparison with linear theory (dashed line).

On the one hand the results obtained at the research pier confirm the anomalous behavior of the celerity spectrum of Sylt island experiment, although in the Black Sea measurements the effect is expressed much weaker. On the other hand the new measurements demonstrate an additional phenomenon. Giant velocity values at low frequencies are obtained together with high coherence values (Fig.10) and almost zero phase shift between points $X = 90 \text{ m}$ and $X = 80 \text{ m}$ mean that the peak at 0.03-

0.04 Hz corresponds to standing waves.

Actually, all points in a standing wave $\xi(x,t) = A \cdot \cos(kx) \cdot \sin(\omega t)$ are in the same phase, hence the celerity should be an infinitely big value.

In conclusion it may be stated that celerity spectra of gravity waves measured in shallow water, offer information on the following phenomena:

- High-frequency anomalous dispersion;
- Low-frequency anomaly at dropping section of energy spectrum;
- Standing waves.

The generalized celerity spectrum for the case of strongly deformed and breaking waves may be presented as in Fig.11. This curve differs significantly from the curve calculated by linear theory.

6. References

Büsching, F., 1978. Wave deformation due to decreasing water depth. Mitteilungen des Leichtweiss-Instituts für Wasserbau der Technischen Universität Braunschweig, 63, pp.168-217.

Büsching, F., 1978. Anomalous dispersion of Fourier components of surface gravity waves in the nearshore area. Proc. 16th Conf. Coastal Engineering, pp.247-267.

Elgar, S., Guza, R.T., 1986. Shoaling gravity waves: comparisons between field observations, linear theory and nonlinear model. Fluid Mech., vol. 158, pp.47-70.

Flick, R.E., Guza, R.T. and Inman, D.L. 1981. Elevation and velocity measurements of laboratory shoaling waves. J.Geophys.Res., 86, pp.4149-4160.

Jenkins, G.M., Watts, D.G. 1968. Spectral analysis and its application. San Francisco: Holden-Day, pp.525.

Kuznetsov, S.Yu., Speranski, N.S. 1990. Phase velocities of free and forced waves in shallow water. In: "Modern processes of sedimentation on shelf", pp.180-186, "Nauka", Moscow, (in Russian).

Lighthill, J., 1978. Waves in fluids. Cambridge Univ. Press, London, pp.504.

Speranski, N.S., 1985. Two types of deformation of wave velocity field in coastal zone. Oceanology, vol. 25, n 6, pp. 723-726.

Thornton, E., Guza, R.T. 1982. Energy saturation and phase speed measured on a natural beach. J. Geophys. Res., C86(5): pp.4149-4160.